Electrochemical sensing of human neutrophil elastase and polymorphonuclear neutrophil activity

Biosensors and Bioelectronics 119 (2018) 209–214

Contents lists available at ScienceDirect

Biosensors and Bioelectronics

journal homepage: www.elsevier.com/locate/bios

Electrochemical sensing of human neutrophil elastase and polymorphonuclear neutrophil activity

Eva González-Fernández[a,1], Matteo Staderini[a,1], Amirah Yussof[a], Emma Scholefield[b], Alan F. Murray[c], Andrew R. Mount[a,*], Mark Bradley[a,*]

[a] EaStCHEM, School of Chemistry, University of Edinburgh, Joseph Black Building, West Mains Road, Edinburgh EH9 3FJ, UK
[b] MRC Centre for Inflammation Research, QMRI, 47 Little France Crescent, Edinburgh EH16 4TJ, UK
[c] School of Engineering, Institute for Bioengineering, The University of Edinburgh, The King's Buildings, Mayfield Road, Edinburgh EH9 3JL, UK

ARTICLE INFO

Keywords:
Self-assembled monolayer
Protease detection
Human neutrophil elastase
Electrochemical detection
Methylene blue-tagged peptides

ABSTRACT

Human neutrophil elastase (HNE) is a serine protease, produced by polymorphonuclear neutrophils (PMNs), whose uncontrolled production has been associated with various inflammatory disease states as well as tumour proliferation and metastasis. Here we report the development and characterisation of an electrochemical peptide-based biosensor, which enables the detection of clinically relevant levels of HNE. The sensing platform was characterised in terms of its analytical performance, enzymatic cleavage kinetics and cross-reactivity and applied to the quantitative detection of protease activity from PMNs from human blood.

1. Introduction

Human neutrophil elastase (HNE), a serine protease secreted by polymorphonuclear neutrophils (PMNs), plays an important role in many physiological and pathological processes (Korkmaz et al., 2008). The proteolytic activity of this enzyme contributes to the body's defence against infectious agents by promoting the destruction of pathogenic bacteria (Meyer-Hoffert and Wiedow, 2011; Nathan, 2006). High levels of unregulated HNE have also been associated with the inflammatory state found in a wide range of acute and chronic diseases (Kolaczkowska and Kubes, 2013; Pham, 2006) with excess HNE causing extracellular matrix degradation, cellular receptor cleavage and healthy tissue disruption (Abe et al., 2009; Chua and Laurent, 2006; Shapiro, 2002). Furthermore, recent studies have suggested a direct role for HNE in promoting tumour proliferation and metastasis (Galdiero et al., 2013; Sato et al., 2006). HNE is therefore a potential diagnostic marker for a number of disease states and detecting it with high sensitivity is clinically important (Henriksen and Sallenave, 2008; Ho et al., 2014; Korkmaz et al., 2010). Common methods to monitor HNE levels rely on immunoassays (de la Rebière de Pouyade et al., 2010; Dunn et al., 1985) and aptamer or peptide-based sensors typically labelled with fluorescent reporters (Avlonitis et al., 2013; Bai et al., 2017; Ferreira et al., 2017; He et al., 2010). In this context, it is interesting to note that electrochemical peptide-based biosensors have proven to be valuable tools for the detection of protease activity (Anne et al., 2012; Liu et al., 2006; Shin et al., 2013; Swisher et al., 2015, 2014, 2013) – as well as a wider range of applications (Huang et al., 2016; Li et al., 2015, 2014; Puiu et al., 2014). Recently, our research group reported an electrochemical peptide-based biosensor which used self-assembled monolayers (SAMs) on gold electrodes for the detection of the model protease trypsin (González-Fernández et al., 2016). This constituted a short peptide sequence, which acts as substrate for the target enzyme, methylene blue as redox reporter and a polyethylene glycol (PEG) spacer that was shown to be important in tuning both the anti-fouling properties and the probe's flexibility (González-Fernández et al., 2018). Upon enzymatic cleavage, a redox-labelled probe fragment is released, leading to a measurable decrease in the electrochemical signal. This system provided a sensitive platform with a clinically relevant limit of detection (LOD) of 250 pM. Building on this approach, here we target the translation of this model system to the detection of HNE in biological (human blood) samples through the development of a novel methylene blue-tagged peptide-based biosensor with an HNE-specific cleavage sequence employing ternary SAMs on a gold surface. This is the first reported example of HNE detection based on a reagent-free labelled electrochemical strategy.

* Corresponding authors.
E-mail addresses: a.mount@ed.ac.uk (A.R. Mount), mark.bradley@ed.ac.uk (M. Bradley).
[1] These authors contributed equally to this study.

https://doi.org/10.1016/j.bios.2018.08.013
Received 1 June 2018; Received in revised form 4 August 2018; Accepted 8 August 2018
Available online 09 August 2018

2. Materials and methods

2.1. Instrumentation

Electrochemical measurements were performed using a conventional three-electrode electrochemical cell driven by a computer-controlled AutoLab PGstat-30 potentiostat running the GPES 4.9 software (EcoChemie, The Netherlands). A platinum wire and a 2 mm diameter polycrystalline gold electrode (IJ Cambria, UK) were used as auxiliary and working electrodes, respectively. All the potentials were referenced to a Ag | AgCl | KCl (3 M) reference electrode (Bioanalytical Systems, Inc., USA). MALDI TOF MS were run on a Bruker Ultraflextreme MALDI TOF/TOF with a matrix solution of sinapic acid (10 mg/mL) in H_2O/CH_3CN/TFA (50/50/0.1).

2.2. Reagents

Human neutrophil elastase, HNE (MW 29.5 kDa) was obtained from Athens Research and Technology Inc. (USA). Cathepsin G, bovine serum albumin (BSA), casein, 6-mercaptohexanol (MCH), 2,2′-(ethylenedioxy) diethanethiol (PDT), HEPES buffer, sodium chloride, sodium acetate were all obtained from Sigma. All reagents were of analytical grade and solutions were prepared using protease-free deionised water. HNE was reconstituted in 50 mM acetate, pH 5.5, with 150 mM NaCl and stored at −80 °C until use.

2.3. Experimental methods

2.3.1. Synthesis

The detailed synthetic experimental procedures are described in Appendix A: Supplementary Data.

2.3.2. Electrode cleaning and pre-treatment

After immersing in the minimum volume of piranha solution (3:1-H_2SO_4 (95%): H_2O_2 (33%)) (CAUTION piranha solution is strongly oxidising and must be handled with care!) for 10 min in order to eliminate any organic matter from the gold surface, the working electrode was successively polished on a polishing cloth using alumina slurries of 1, 0.3 and 0.05 μm particle size (Buehler, Germany). Afterwards, this electrode was further cleaned by immersion in H_2SO_4 (95%) and then HNO_3 (65%) at room temperature for 10 min. Finally, the working electrode was subjected to cyclic voltammetry, carrying out potential cycles between 0 and + 1.6 V in 0.1 M H_2SO_4 at a scan rate of 100 mV s^{-1} until the characteristic voltammogram of clean polycrystalline gold was obtained.

2.3.3. Sensing phase preparation protocol

The sensing phase was formed as a mixed SAM on the gold electrode surface by immersing the freshly cleaned and pre-treated gold working electrode overnight at 4 °C in a 40 μM ethanolic solution of the appropriate redox-labelled peptide (substrate, composed of L-amino acids; or control, with all amino acids replaced with their respective D-amino acid analogues) and freshly prepared PDT (600 μM). After washing with ethanol, the resulting SAM-modified electrode was immersed in 1 mM MCH in ethanol for 1 h at room temperature. Finally, two washing steps were carried out, firstly in ethanol and then in HEPES buffer (50 mM HEPES, 150 mM NaCl, pH 7.4). The modified electrodes were stored in HEPES buffer at 4 °C until use.

2.3.4. Sensor measurements

The modified electrodes were immersed in HEPES buffer and electrochemically interrogated using square wave voltammetry (SWV, at a frequency of 60 Hz and with an amplitude of 25 mV and a step potential of 5 mV) until a stable signal was obtained. After addition of the target enzyme, the SWV signal was continuously monitored with time, with the resulting signal decrease being expressed as the relative change in SWV peak current with respect to the initial peak current (henceforth shown as a negative % signal change).

2.3.5. Blood sample treatment for activated/non-activated PMNs

Freshly isolated PMNs – obtained from healthy donors following the blood preparation protocol previously described (Avlonitis et al., 2013) – were re-suspended at 2×10^6 cells/mL in PBS containing 0.9 mM Ca^{2+} and 0.5 mM Mg^{2+}. The sample was divided in two tubes, and to one of them A23187 (a calcium ionophore, 10 μM final concentration) was added in order to activate the PMNs. The other one was kept non-activated as a negative control. Both tubes were heated at 37 °C for 10 min in a water bath and then centrifuged for 5 min. The cell pellet was discarded and the supernatant stored at −20 °C until use.

3. Results and discussion

The sensing platform was based on the immobilisation of a redox-labelled peptide sequence, which contained a specific cleavage site for the enzyme, on a gold surface as a SAM. The peptide sequence (APEEIMRRQ) has been reported as a highly specific HNE cleavable sequence in a fluorescent assay for HNE detection (Avlonitis et al., 2013). A novel peptide probe has been designed and synthesised, adding further functionality to this previously reported sequence. In order to generate an HNE electrochemical probe, a methylene blue redox tag was attached to the amino-terminus of the peptide with the addition of a 2-unit ethylene glycol moiety (PEG-2) and a cysteine at the carboxy-terminus, which enables facile SAM immobilisation of the probe through the formation of a S-Au bond (Fig. 1A). A probe containing the equivalent non-cleavable D-amino acid sequence was also synthesised as a negative control probe. The sensing mechanism relies on specific enzyme-catalysed cleavage followed by the release of the labelled peptide fragment from the SAM-modified gold surface into solution (Fig. 1B). This results in a decrease of the electrochemical signal, which is interrogated before and during enzyme exposure by square wave voltammetry (SWV) and presented as a negative % signal change (a decrease in the relative peak SWV current with respect to the initial value recorded before enzyme addition). The cleavage site, immediately after the methionine residue, was confirmed in solution through cleavage fragment mass analyses by MALDI-TOF MS (Fig. S1). The sensing surfaces were generated using a previously optimised ternary-SAM (T-SAM) configuration (González-Fernández et al., 2016) established as showing enhanced SAM biosensing, according to the protocol detailed in Section 2.3.2. This is denoted a ternary-SAM as it is composed of 3 different thiols on the gold surface: the peptide-probe, a co-adsorbed pegylated dithiol and mercaptohexanol.

3.1. Analytical performance against varying HNE concentrations

Substrate-modified gold electrodes were prepared and their performance evaluated upon immersion in solutions containing varying HNE concentrations (10–150 nM). The modified-electrodes were electrochemically interrogated by SWV in real-time when exposed to different HNE concentrations (Fig. 2). As shown in Fig. 2A the presence of HNE caused a decrease of the % signal, and as expected, the higher the HNE concentration the faster the % signal change recorded, resulting from faster proteolytic cleavage of the SAM-modified surface; where the (negative) % signal change $= (I_{SWV}(t) - I_{SWV}(t = 0))/ I_{SWV}(t = 0) \times 100$, with I_{SWV} ($t = 0$) defined as the signal recorded before the addition of the enzyme. As previously observed for other SAM systems, the signal did not decrease by 100%, suggesting that a subset of the immobilised peptides are not available for cleavage, which has been previously attributed to polycrystalline gold roughness leading to site inaccessibility (González-Fernández et al., 2018). Furthermore, additional cyclic voltammetry was performed in order to calculate the change of surface coverage of active methylene blue-peptide upon HNE incubation (100 nM), which showed the expected decrease, consistent

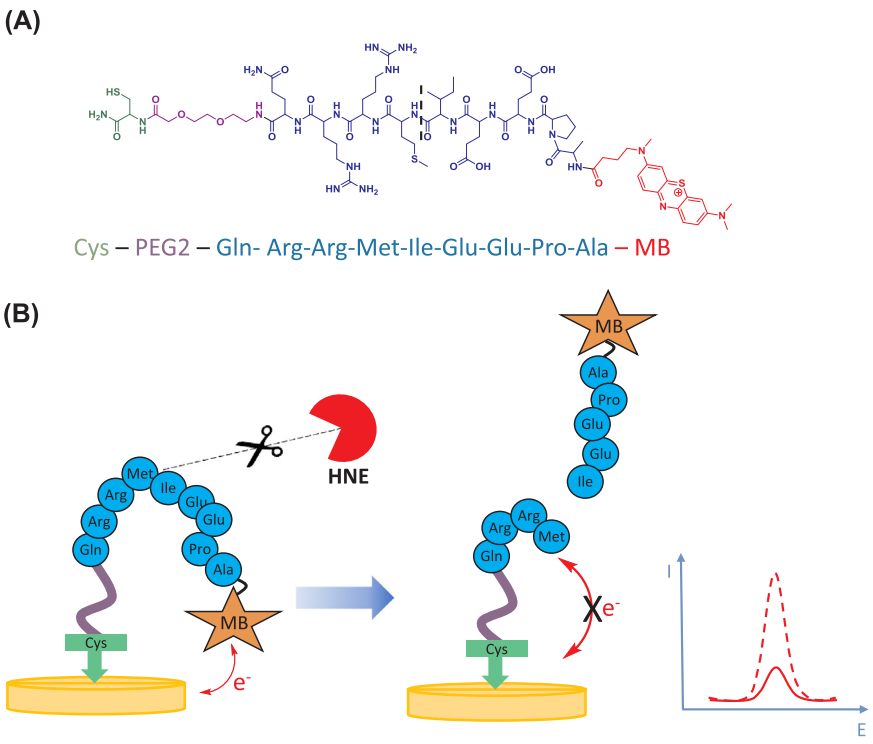

Fig. 1. (A) Structure of the methylene blue-tagged peptide probe for HNE. (B) Principle of detection for the peptide-based electrochemical biosensor. HNE catalyses the cleavage of the methylene blue-labelled peptide substrate releasing the redox containing fragment into solution, leading to a decrease in the electrochemical signal as measured by SWV.

with the SWV data (Fig. S2, Supplementary material). It is interesting that the signal value, *A*, at the end of the measurements (90 min); where *A* is the normalised signal at time *t*, calculated readily from the data as $A(t)$ = (% signal change (*t*)) / (% signal change at long times ($t \rightarrow \infty$)) and at high HNE concentration (150 nM)) varies linearly with HNE concentration (Fig. 2B) and shows a dynamic range for sensing up to 100 nM. The limit of detection (LOD) after 90 min was determined to be 4 nM, calculated as the protease concentration corresponding to the % signal change equal to that of the blank signal ([HNE] = 0 nM) minus 3 × SD, where SD is the standard deviation for the blank. Although this is a facile single point measurement and analysis, which should be prone to relatively large error, it is interesting that this value is lower than previously reported values for a peptide-labelled fluorescence assay (Ferreira et al., 2017) and a peptide-based assay with quartz crystal microbalance (QCM) detection (Stair et al., 2009), but still higher than those reported for assays using antibodies or aptamers (Bai et al., 2017; Dunn et al., 1985; He et al., 2010), which however, also require several incubations and/or washing steps as opposed to the proposed platform (see comparison in Table S1, Supplementary material). Furthermore, the platform showed good reproducibility, with a 5% coefficient of variation (n = 3) for 100 nM HNE. Interestingly, this covers the clinically relevant range previously reported for HNE levels in moderate and severe pneumonia, 4–10 nM, respectively (Matsuse et al., 2007). It should be noted that for such single point measurements the choice of time at which the measurement is taken can be selected in order to tune the requirements of the particular sensing application. As shown in Fig. S3, measuring at a longer time allows enhanced discrimination in the lower part of the enzyme concentration range. On the other hand, at shorter times, i.e. 8 min, a good sensing performance in the higher part of the concentration range was observed. Examples of the square wave voltammograms obtained for 100 nM HNE at different times are shown in Fig. 2C.

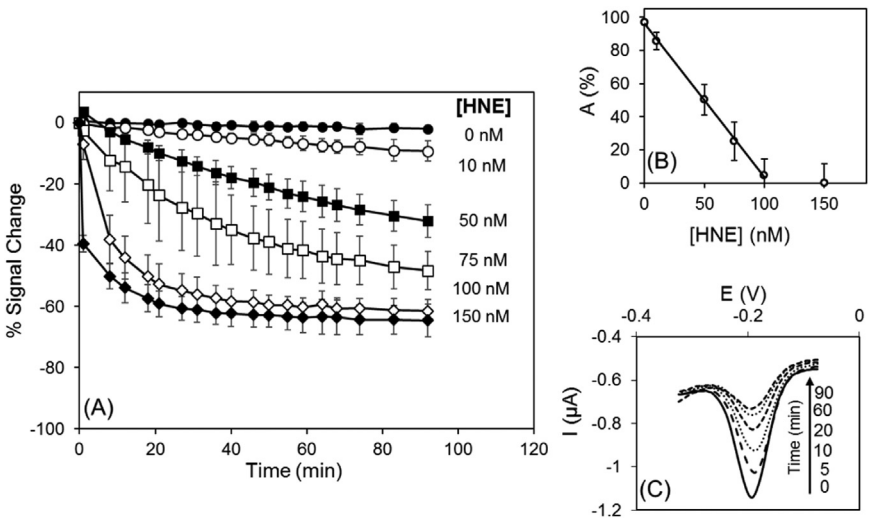

Fig. 2. Electrochemical detection of HNE. (A) % Signal change-time course for substrate-modified electrodes immersed in varying HNE concentrations (0, 10, 50, 75, 100 and 150 nM) in HEPES buffer. (B) Adjusted signal, *A* (%), after 90 min plotted against the concentration of HNE. The straight line corresponds to the best linear fit (%S = −0.92 [HNE] (nM) + 95.92; r^2 = 0.99). (C) SWV curves registered at different incubation times (0, 5, 10, 20, 60 and 90 min) for 100 nM HNE in HEPES buffer. All data points represent the average and standard deviation for typically 3 individual sensing phases.

3.2. Kinetic analysis of enzymatic cleavage

As an alternative to analysis of data collected at selected individual times, which is subject to a relatively large error, the % signal decrease registered for the varying HNE concentrations as a function of time was measured and analysed using a Michaelis-Menten kinetic model previously established for an equivalent sensing platform for the protease trypsin (González-Fernández et al., 2016). The fraction of cleavable peptide cleaved at time t ($\theta(t) = 1 - A(t)$) was plotted as a function of time (t) and fitted to the previously reported model through the equation:

$$\theta = 1\text{–}e^{-kt}, \text{ or } A = e^{-kt}, \quad (1)$$

where k is the effective cleavage rate constant. As shown in Fig. S4, good fits were obtained for HNE concentrations up to 75 nM, whereas poorer fits were obtained for higher concentrations (100 and 150 nM) using this model. It can be seen that the origin of this deviation from the proposed model is the fast signal change recorded at higher concentrations of HNE; after enzyme addition, there is an initial rapid drop on the registered electrochemical signal, which is followed by a slower decrease. The second slower step is attributed to the following enzyme cleavage step. In order to prove this hypothesis, longer time data from Fig. 2A, were fitted to the above model, which allows choice of the initial time, t_0, and value of A, A_0, such that,

$$A = A_0 \exp(-k(t - t_0)). \quad (2)$$

As shown in Fig. 3A, fitting these data from Fig. 2A starting at t_0 = 8 min to Eq. (2) generated good fits across the entire enzyme concentration range tested. The fit allowed extraction of a k value for each of the HNE concentrations. We speculate that this initial signal drop, which is increasingly apparent at enzyme concentrations above 100 nM, originates from an initial adsorption of a near monolayer of the enzyme onto the sensor surface through enzyme-substrate binding at these relatively large peptide-substrate surface concentrations, which inhibits peptide flexibility and hinders the approach of the redox tag to the electrode surface, thereby decreasing the peak current without resulting in cleavage. It is interesting that the dependence of k on the HNE concentration did not follow the previously observed hyperbolic performance for an analogue sensing platform for trypsin. We speculate that this kinetic behaviour could arise from the formation of a near monolayer of protease that slowly cleaves the surface-immobilised labelled-peptide at a constant rate. In the low protease concentration range, an increase on the amount of enzyme leads to a higher amount of protease bound to the substrate-modified surface, as determined by the affinity constant. The observed increase in the cleavage rate is then due to the increase in surface bound HNE, each of which progressively cleaves surface peptide at a constant rate. An increase on the cleavage rate is then registered until a closely packed bound protease surface layer is formed, which occurs at a relatively low point on the binding curve (low number of surface peptides bound) due to the massive difference between the size of HNE and surface-bound probe. At this point (HNE concentrations greater than 100 nM) the surface is saturated with a monolayer of HNE, leading to a constant cleavage rate. This is similar to, and consistent with, previously reported data on a surface-based enzymatic amplification processes for enhanced sensing which employed streptavidin-biotin binding of the large protein and subsequent insoluble product deposition (Kaatz et al., 2012).

3.3. Selectivity study

The sensing platform was assessed in terms of selectivity towards HNE in comparison with potential interferences from real samples (i.e. from other components of the sample). Both substrate and control-modified surfaces were exposed to different solutions containing cathepsin G (100 nM), a serine protease also present in PMNs; BSA (100 nM) and casein (100 nM) as means of evaluating non-specific interactions; and ions such as calcium (1 mM). The electrochemical SWV signal was monitored for 90 min and the final value plotted as % signal change. As shown in Fig. 4A, the sensing platform exhibited low cross-reactivity against non-specific proteins (BSA and casein), which is consistent with the ability of such T-SAMs to enhance anti-fouling properties (Campuzano et al., 2011; González-Fernández et al., 2016). It is worth noting that cross-reactivity against cathepsin G was observed, with the substrate-modified surface showing a 27% signal change in presence of 100 nM cathepsin G, constituting about half of the signal registered for the same concentration of HNE. The control-modified surface showed no cleavage with either HNE or cathepsin G. An equivalent output was obtained when assessing the HNE/cathepsin G selectivity in terms of peptide cleavage rate from the electrode surface (Fig. S5), Fitting to Eq. (2) allowed extraction of a k of $0.032 \pm 0.003\ min^{-1}$, which is half of the value obtained for the same concentration of HNE, $0.064 \pm 0.003\ min^{-1}$. These results contrast with the high selectivity shown in an analogous fluorescent system based on the same peptide sequence, and confirmed in solution for the substrate probe used in this study (Fig. S1, Supplementary material), which can perhaps be attributed to the likelihood that the immobilisation of the probe as an oriented, densely packed layer on a solid support can also modify the peptide's binding and recognition properties. Indeed, the presence of arginine residues in the peptide sequence could be the source of such cross-reactivity, as cathepsin G has been described to cleave after positively-charged residues (Korkmaz et al., 2011). We speculate that, the orientation of the immobilised peptide on the electrode surface could enhance the importance of these arginine residues on the recognition event with cathepsin G. It should be noted that this cross-reactivity does not impede the application of the proposed sensing platform to detecting PMN activity in blood samples, as cathepsin G is also simultaneously released from activated PMNs.

The presence of calcium ions (1 mM) was seen to produce a small

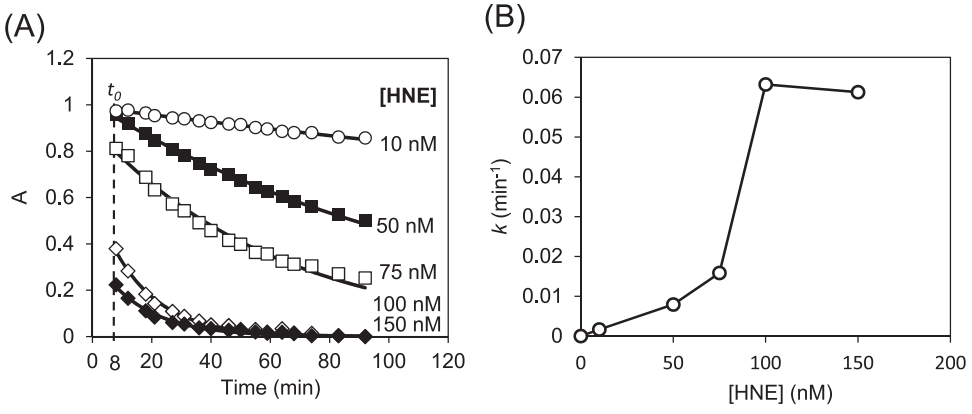

Fig. 3. (A) Fractional cleavage vs time plot for substrate-modified electrode cleavage from Fig. 2A upon immersion in different HNE concentrations, being t_0 = 8 min. Solid lines represent the best non-linear fit according to Eq. (2). (B) Variation of the effective constant rate, k, obtained from fitting the data as a function of the HNE concentration. Each of the points represent k values obtained from fittings to Eq. (2) shown in Fig. 3A.

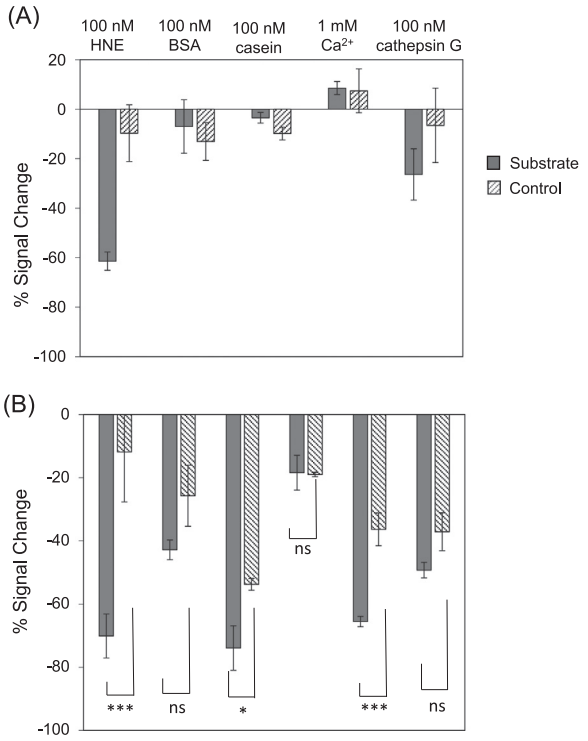

Fig. 4. % Signal change registered for both substrate- (grey columns) and control-modified (patterned columns) electrodes after 90 min incubation with (A) HNE (100 nM), BSA (100 nM), casein (100 nM), Ca^{2+} (1 mM) and cathepsin G (100 nM) in 50 mM HEPES buffer; (B) (+) activated/(-) non-activated PMNs from pre-treated blood samples from 3 different healthy donors (D1–3). *** $P < 0.01$; * $P < 0.1$; ns = non-significant by one-way ANOVA with Tukey post-test. All values correspond to average and standard deviation of typically 3 individual modified-electrodes.

increase in the SWV signal, perhaps arising from complexation of the PEG-based spacer and/or the glutamic acid residues with the Ca^{2+} ions, which could bring the redox tag closer to the electrode surface and thus, enhance the probability of electron transfer.

3.4. Sensing HNE in real samples from human blood

HNE (and cathepsin G) is secreted by PMNs, the most abundant blood leukocytes (Di Carlo et al., 2001). The sensing platform was therefore challenged with activated PMNs from human blood as a means of interrogating its ability to work in a clinically relevant setting. Non-activated PMNs were used as a negative control. Blood samples from 3 different healthy donors were processed following the protocol detailed in Section 2.3.4 in order to activate (+) /non-activate (-) PMNs, which leads to the release/non-release of HNE. Both substrate- and control-modified electrodes were immersed in each sample and the SWV registered in real-time. Plotting the % signal change after 90 min for both surfaces enabled a clear discrimination between the activated ((+)–HNE) and non-activated ((-)–HNE) samples for all 3 donors (Fig. 4B). Indeed, for each tested donor the % signal change registered for both substrate and control surfaces was significantly different for the (+)–HNE samples, in contrast to the non-significant difference found for (-)–HNE ones. There was a slight difference in performance for the 3 samples tested, attributable to natural donor-to-donor variability and the presence of endogenous HNE (e.g. donors with low level infection) or to slight variability of blood preparation causing activation of the PMNs. Additionally, the performance of the sensing platform for both substrate and control-modified surfaces in real samples was subjected to kinetic analysis, fitting the registered signal to Eq. (2). Fig. S6 shows the fittings for the 3 samples tested, and the extracted k values

Table 1
Values of k (min^{-1}) obtained from fitting Eq. (2) to the data registered for substrate- and control-modified surfaces upon immersion in activated/non-activated real samples for 3 donors.

Donor No. (Activated/non-activated)	k (min^{-1}) for substrate	k (min^{-1}) for control
Donor-1 (Activated)	0.076 ± 0.003	− 0.0047 ± 0.0005
Donor-1 (Non-activated)	0.014 ± 0.002	0.004 ± 0.002
Donor-2 (Activated)	0.051 ± 0.002	0.004 ± 0.002
Donor-2 (Non-activated)	0.0029 ± 0.0004	0.0023 ± 0.0004
Donor-3 (Activated)	0.026 ± 0.003	0.0010 ± 0.0004
Donor-3 (Non-activated)	0.016 ± 0.004	0.0058 ± 0.0009

are summarised in Table 1. From these data we concluded that kinetic analysis also allows discrimination between the activated and the non-activated samples, as extracted k values for the substrate- and control-modified surfaces corresponding to the activated samples differ by an order of magnitude in all cases, meaning that the HNE cleavage leads a significant and measurable signal. On the other hand, for non-activated samples, registered k values for substrate and control-modified surfaces were of the same order of magnitude, indicating that the effect of the small signal decrease registered (probably due to non-specific adsorption of species from these complex samples onto the modified surface) is not significant.

4. Conclusions

We report a peptide-based electrochemical biosensor for the specific detection of the serine protease HNE. The platform was based on the immobilisation, via a SAM, of a methylene blue-labelled peptide sequence, that acts as substrate for the enzyme. Enzymatic cleavage leads to release of the redox reporter and a decrease of the electrochemical signal, as measured by SWV. The proposed system enabled clinically relevant HNE detection between 10 and 150 nM through analysing the signal change as a function of time following a Michaelis-Menten based kinetic model. High selectivity towards the target enzyme was achieved when compared to non-specific proteins although, a degree of cross-reactivity was observed for a related serine protease, cathepsin G, attributed to differences in the oriented surface-bound target probe, perhaps originating from the arginine residues within the target probe sequence. A D-amino acid peptide analogue was used as negative control for all measurements and showed no activation. Finally, the sensing platform was successfully applied for sensing HNE and cathepsin G activity from PMNs isolated from human blood, enabling discrimination between activated and un-activated polymorphonuclear neutrophils in clinically relevant samples.

Acknowledgements

Implantable Microsystems for Personalised Anti-Cancer Therapy is a EPSRC (Engineering and Physical Sciences Research Council, UK) funded grant (Ref. EP/K034510/1)

Ethics approval to take whole blood from healthy volunteers was obtained from the local Lothian Research Ethics Committee. Study title - The Role of Inflammation in Human Immunity (AMREC Reference number 15-HV-013).

Data used within this publication can be accessed at: http://dx.doi.org/10.7488/ds/2409.

Appendix A. Supplementary material

Supplementary data associated with this article can be found in the online version at doi:10.1016/j.bios.2018.08.013.

References

Abe, T., Usui, A., Oshima, H., Akita, T., Ueda, Y., 2009. A pilot randomized study of the neutrophil elastase inhibitor, Sivelestat, in patients undergoing cardiac surgery. Interact. Cardiovasc. Thorac. Surg. 9 (2), 236–240.

Anne, A., Chovin, A., Demaille, C., 2012. Optimizing electrode-attached redox-peptide systems for kinetic characterization of protease action on immobilized substrates. observation of dissimilar behavior of trypsin and thrombin enzymes. Langmuir 28 (23), 8804–8813.

Avlonitis, N., Debunne, M., Aslam, T., McDonald, N., Haslett, C., Dhaliwal, K., Bradley, M., 2013. Highly specific, multi-branched fluorescent reporters for analysis of human neutrophil elastase. Org. Biomol. Chem. 11 (26), 4414–4418.

Bai, Y., Wang, H., Zhao, Q., 2017. Detection of human neutrophil elastase by aptamer affinity capillary electrophoresis coupled with laser-induced fluorescence using specified site fluorescently labeled aptamer. Anal. Bioanal. Chem. 409 (29), 6843–6849.

Campuzano, S., Kuralay, F., Lobo-Castañón, M.J., Bartošík, M., Vyavahare, K., Paleček, E., Haake, D.A., Wang, J., 2011. Ternary monolayers as DNA recognition interfaces for direct and sensitive electrochemical detection in untreated clinical samples. Biosens. Bioelectron. 26 (8), 3577–3583.

Chua, F., Laurent, G.J., 2006. Neutrophil elastase. Proc. Am. Thorac. Soc. 3 (5), 424–427.

de la Rebière de Pouyade, G., Franck, T., Salciccia, A., Deby-Dupont, G., Grulke, S., Heyden, L.V., Sandersen, C., Serteyn, D., 2010. Development of an enzyme-linked immunosorbent assay for equine neutrophil elastase measurement in blood: Preliminary application to colic cases. Vet. Immunol. Immunopathol. 135 (3), 282–288.

Di Carlo, E., Forni, G., Lollini, P., Colombo, M.P., Modesti, A., Musiani, P., 2001. The intriguing role of polymorphonuclear neutrophils in antitumor reactions. Blood 97 (2), 339.

Dunn, T.L., Blackburn, W.D., Koopman, W.J., Heck, L.W., 1985. Solid-phase radioimmunoassay for human neutrophil elastase: a sensitive method for determining secreted and cell-associated enzyme. Anal. Biochem. 150 (1), 18–25.

Ferreira, A.V., Perelshtein, I., Perkas, N., Gedanken, A., Cunha, J., Cavaco-Paulo, A., 2017. Detection of human neutrophil elastase (HNE) on wound dressings as marker of inflammation. Appl. Microbiol. Biot. 101 (4), 1443–1454.

Galdiero, M.R., Bonavita, E., Barajon, I., Garlanda, C., Mantovani, A., Jaillon, S., 2013. Tumor associated macrophages and neutrophils in cancer. Immunobiology 218 (11), 1402–1410.

González-Fernández, E., Avlonitis, N., Murray, A.F., Mount, A.R., Bradley, M., 2016. Methylene blue not ferrocene: optimal reporters for electrochemical detection of protease activity. Biosens. Bioelectron. 84, 82–88.

González-Fernández, E., Staderini, M., Avlonitis, N., Murray, A.F., Mount, A.R., Bradley, M., 2018. Effect of spacer length on the performance of peptide-based electrochemical biosensors for protease detection. Sens. Actuators B: Chem. 255, 3040–3046.

He, J.-L., Wu, Z.-S., Zhang, S.-B., Shen, G.-L., Yu, R.-Q., 2010. Fluorescence aptasensor based on competitive-binding for human neutrophil elastase detection. Talanta 80 (3), 1264–1268.

Henriksen, P.A., Sallenave, J.-M., 2008. Human neutrophil elastase: mediator and therapeutic target in atherosclerosis. Int. J. Biochem. Cell Biol. 40 (6), 1095–1100.

Ho, A.-S., Chen, C.-H., Cheng, C.-C., Wang, C.-C., Lin, H.-C., Luo, T.-Y., Lien, G.-S., Chang, J., 2014. Neutrophil elastase as a diagnostic marker and therapeutic target in colorectal cancers. Oncotarget 5 (2), 473–480.

Huang, Y., Li, H., Fan, Q., Wang, L., Wang, Y., Li, G., 2016. Multifunctional nanocatalyst-based ultrasensitive detection of human tissue transglutaminase 2. Biosens. Bioelectron. 83, 85–90.

Kaatz, M., Schulze, H., Ciani, I., Lisdat, F., Mount, A.R., Bachmann, T.T., 2012. Alkaline phosphatase enzymatic signal amplification for fast, sensitive impedimetric DNA detection. Analyst 137 (1), 59–63.

Kolaczkowska, E., Kubes, P., 2013. Neutrophil recruitment and function in health and inflammation. Nat. Rev. Immunol. 13, 159.

Korkmaz, B., Horwitz, M.S., Jenne, D.E., Gauthier, F., 2010. Neutrophil Elastase, Proteinase 3, and Cathepsin G as Therapeutic Targets in Human Diseases. Pharmacol. Rev. 62 (4), 726–759.

Korkmaz, B., Jégot, G., Lau, L.C., Thorpe, M., Pitois, E., Juliano, L., Walls, A.F., Hellman, L., Gauthier, F., 2011. Discriminating between the activities of human cathepsin G and chymase using fluorogenic substrates. FEBS J. 278 (15), 2635–2646.

Korkmaz, B., Moreau, T., Gauthier, F., 2008. Neutrophil elastase, proteinase 3 and cathepsin G: physicochemical properties, activity and physiopathological functions. Biochimie 90 (2), 227–242.

Li, H., Huang, Y., Yu, Y., Li, W., Yin, Y., Li, G., 2015. Peptide-based method for detection of metastatic transformation in primary tumors of breast cancer. Anal. Chem. 87 (18), 9251–9256.

Li, Y., Afrasiabi, R., Fathi, F., Wang, N., Xiang, C., Love, R., She, Z., Kraatz, H.-B., 2014. Impedance based detection of pathogenic E. coli O157:H7 using a ferrocene-antimicrobial peptide modified biosensor. Biosens. Bioelectron. 58, 193–199.

Liu, G., Wang, J., Wunschel, D.S., Lin, Y., 2006. Electrochemical Proteolytic Beacon for Detection of Matrix Metalloproteinase Activities. J. Am. Chem. Soc. 128 (38), 12382–12383.

Matsuse, H., Yanagihara, K., Mukae, H., Tanaka, K., Nakazato, M., Kohno, S., 2007. Association of plasma neutrophil elastase levels with other inflammatory mediators and clinical features in adult patients with moderate and severe pneumonia. Resp. Med. 101 (7), 1521–1528.

Meyer-Hoffert, U., Wiedow, O., 2011. Neutrophil serine proteases: mediators of innate immune responses. Curr. Opin. Hematol. 18 (1), 19–24.

Nathan, C., 2006. Neutrophils and immunity: challenges and opportunities. Nat. Rev. Immunol. 6, 173.

Pham, C.T.N., 2006. Neutrophil serine proteases: specific regulators of inflammation. Nat. Rev. Immunol. 6, 541.

Puiu, M., Idili, A., Moscone, D., Ricci, F., Bala, C., 2014. A modular electrochemical peptide-based sensor for antibody detection. Chem. Commun. 50 (64), 8962–8965.

Sato, T., Takahashi, S., Mizumoto, T., Harao, M., Akizuki, M., Takasugi, M., Fukutomi, T., Yamashita, J.-i., 2006. Neutrophil elastase and cancer. Surg. Oncol. 15 (4), 217–222.

Shapiro, S.D., 2002. Neutrophil elastase. Am. J. Resp. Cell Mol. Biol. 26 (3), 266–268.

Shin, D.-S., Liu, Y., Gao, Y., Kwa, T., Matharu, Z., Revzin, A., 2013. Micropatterned Surfaces functionalized with electroactive peptides for detecting protease release from cells. Anal. Chem. 85 (1), 220–227.

Stair, J.L., Watkinson, M., Krause, S., 2009. Sensor materials for the detection of proteases. Biosens. Bioelectron. 24, 2113–2118.

Swisher, L.Z., Prior, A.M., Gunaratna, M.J., Shishido, S., Madiyar, F., Nguyen, T.A., Hua, D.H., Li, J., 2015. Quantitative electrochemical detection of cathepsin B activity in breast cancer cell lysates using carbon nanofiber nanoelectrode arrays toward identification of cancer formation. Nanomed.-Nanotechnol. 11, 1695–1704.

Swisher, L.Z., Prior, A.M., Shishido, S., Nguyen, T.A., Hua, D.H., Li, J., 2014. Quantitative electrochemical detection of cathepsin B activity in complex tissue lysates using enhanced AC voltammetry at carbon nanofiber nanoelectrode arrays. Biosens. Bioelectron. 56, 129–136.

Swisher, L.Z., Syed, L.U., Prior, A.M., Madiyar, F.R., Carlson, K.R., Nguyen, T.A., Hua, D.H., Li, J., 2013. Electrochemical protease biosensor based on enhanced ac voltammetry using carbon nanofiber nanoelectrode arrays. J. Phys. Chem. C 117, 4268–4277.